International Journal of Industrial Engineering, 32(6), 1478-1486, 2025

A TIME SERIES CONTROL CHART FOR MONITORING ABNORMAL BLOOD GLUCOSE LEVELS

Naarpa Kuntapa and Ussaneei Purintrapiban*

Department of Production Engineering
King Mongkut's University of Technology Thonburi (KMUTT)
Bangkok, Thailand
*Corresponding author's e-mail: ussaneei.pur@kmutt.ac.th

Global diabetes statistics indicate a continuous rise in prevalence and complications, highlighting the need for more effective monitoring and management strategies. Selecting techniques for monitoring blood glucose levels is essential in detecting abnormalities, identifying root causes, and facilitating behavioral adjustments. This study proposes a control chart constructed by using a robust estimator concept, which is suitable for monitoring the autocorrelated blood glucose data as a time-series control chart based on σ_{ARMA}. Its performance is evaluated by using a Monte Carlo simulation under varying parameters and compared with existing charts based on the average run length. Results will show that the proposed chart is the quickest in detecting abnormalities when the data are highly correlated and performs comparably in medium-to-low correlations. It is also applied to real patient self-monitoring data and interpreted with treatment guidelines to support behavioral adjustment. A case study will confirm its capability, particularly when used with physician guidance. The proposed chart provides timely behavior-linked insights, enhancing diabetes management.

Keywords: Autocorrelation, Control chart, Diabetes, Self-management, Time series.

(Received on July 16, 2025; Accepted on November 15, 2025)

1. INTRODUCTION

Type 2 diabetes (T2D) is a growing global health concern, affecting 588.7 million people in 2024. By 2050, this number is projected to reach 852.5 million, highlighting a worsening public health crisis (IDF Diabetes Atlas, 2025). T2D is a multifactorial disease linked to genetic and environmental factors, including sedentary lifestyles, poor diet, smoking, alcohol consumption, and inadequate self-care (Sapkota *et al*., 2018). Many individuals remain unaware of its severity. Essential resources are often lacking, health monitoring is insufficient, medication adherence is low, and lifestyle adjustments are limited. These gaps increase the risk of severe complications and mortality (American Diabetes Association Professional Practice Committee, 2025). Regular blood glucose monitoring is crucial for effective diabetes management. This enables real-time adjustments in diet, medication, and lifestyle to maintain optimal glycemic levels. Although the self-monitoring of blood glucose (SMBG) provides behavioral insights, analysis techniques are often insufficient, leading to overlooked beneficial behaviors, elevated blood glucose levels, and increased health risks. Furthermore, misconceptions about relevant health information are common, resulting in poor healthcare decisions (Siqueira *et al*., 2015).

Among the various monitoring techniques, control charts are widely applied in healthcare (Kao, 2013; Hamm et al., 2024; Aslam *et al*., 2024), particularly in diabetes management. Control charts are used to monitor glucose fluctuations over time and support clinical practice (Pakdil *et al*., 2019; Aslam *et al*., 2019; Atieno Wagoro *et al*., 2020). A visual representation of trends enables the early detection of abnormalities and the timely intervention by healthcare professionals.

Traditional control charts are fundamentally based on the assumption that process data are independent and identically distributed (IID). However, this assumption often does not hold true in real-world applications. In particular, data obtained from SMBG frequently exhibit serial correlation, where current measurements are influenced by preceding values. This autocorrelation makes traditional control charts unsuitable for such data, potentially leading to false alarms or missed detections. Even low levels of autocorrelation can significantly impact chart performance, particularly under conditions involving abrupt disturbances (Prajapati and Singh, 2012). Recognizing these limitations, various studies have proposed improvements to traditional control charts. One approach involves filtering out autocorrelation and monitoring only the pure residuals. Although this approach is relatively simple and has demonstrated effectiveness in detecting large process shifts (Haridy and Benneyan, 2024), it still faces limitations in promptly identifying small changes and suffers from errors when autocorrelation is present, which may result in misleading conclusions (Prajapati and Singh, 2012).

DOI: 10.23055/ijietap.2025.32.6.11211 **ISSN 1072-4761**

Subsequently, researchers have developed control charts that directly incorporate autocorrelated data by using alternative estimators. The underlying idea in these studies is to fit an appropriate time-series model to the correlated structure. Focusing on healthcare applications, Siqueira *et al*. (2015) presented a control chart based on a forecast model, and the mean absolute deviation (MAD) was selected for estimating the standard deviation. According to research findings, the behaviors of the plotted points on the charts appear more sensitive in detecting abnormality in the case of autocorrelated data. The time-series control chart with MAD can quickly detect all magnitudes of change in the process mean shift, but it also provides false alarms (Kuntapa and Purintrapiban, 2019). This limitation arises from a property of MAD, which is not a good estimator of standard deviation, particularly for autocorrelated data. MAD considers only the size of the error without accounting for its polarity (Yager and Alajlan, 2014).

Due to this inappropriate estimation of the standard deviation, the chart's performance is negatively affected (Faria *et al*., 2020). Since the estimator plays a crucial role in determining the chart's effectiveness, further refinement may be required to enhance its reliability (Montgomery, 2020). Given the limitations of the estimator and the impact on chart performance, a more robust approach is required. Thus, the control chart developed in this study is based on the concept of a good estimator, which must be (i) unbiased, (ii) consistent, (iii) efficient, and (iv) sufficient, as detailed in the work by Babatunde *et al*. (2020).

Building upon this objective, this study aims to develop a suitable control chart for monitoring blood glucose levels, using an appropriate estimator of standard deviation, i.e., a time-series control chart based on σ_{ARMA}. To achieve this aim, the following section presents the proposed control chart and describes its construction and key principles. Therefore, this study addresses the identified research gap by introducing a control chart specifically designed for autocorrelated blood glucose data. This approach enhances monitoring reliability and detection performance. The proposed method, which is referred to as a time-series control chart based on σ_{ARMA}, aims to rapidly detect abnormal events or behavioral changes. Its performance is evaluated by comparing the average run length (ARL) with those of existing approaches. Furthermore, the chart provides actionable insights when applied in a case study involving real-world situations. Plotting the SMBG data into the chart, followed by analysis and interpretation, supports self-management and adaptation to lifestyle modifications.

2. METHODOLOGY

The blood glucose levels are autocorrelated because the level of blood glucose on the current day is related to the levels on the previous days. This assumption is based on a stationary process. This implies that diabetic patients have well-controlled blood glucose levels, with fluctuations remaining within a stable range over time. Hence, this study focuses on a stationary process of the autoregressive moving (ARMA) (*p*, q) model, where *p* = 1 and *q* = 1, as described in Equation (1). The variance of the ARMA (1, 1) process is given by Equation (2). This standard deviation estimator is formally defined as the square root of the variance derived from the fitted ARMA (1,1).

$$X_t = \delta + \phi_1 X_{t-1} - \theta_1 \varepsilon_{t-1} + \varepsilon_t \tag{1}$$

$$\sigma_{X_t}^2 = \left(\frac{1 + {\theta_1}^2 - 2\phi_1\theta_1}{1 - \phi_1^2}\right)\sigma_\varepsilon^2 \tag{2}$$

$$\sigma_{X_t} = \sqrt{\sigma_{X_t}^2} \tag{3}$$

where the ARMA (*p*, *q*) model consists of two parts that are based on the autoregressive process (AR(*p*)) and the moving average process (MA(*q*)). An ARMA process can be written more concisely by defining associated polynomials in the lag operator, as expressed in the work by Box *et al*. (2016). The current disturbance term depends on the lagged disturbances, where δ is the constant, $X_{t-1}, X_{t-2}, \ldots, X_{t-p}$ are response variables at a lag of time, and the residual at time t is ε_t with $E(\varepsilon_t) = 0$ and $Var(\varepsilon_t) = \sigma_\varepsilon^2$. The coefficients of AR are $\phi_1, \phi_2, \ldots, \phi_p$ with $|\phi| < 1$ and the coefficients of MA are $\theta_1, \theta_2, \ldots, \theta_q$ with $|\theta| < 1$and are associated with $\varepsilon_{t-1}, \varepsilon_{t-2}, \ldots, \varepsilon_{t-q}$, respectively. All model parameters are estimated by using computational methods, including maximum likelihood estimation (MLE). Further details on the estimation procedures can be found in the work by Box *et al*. (2016)

The concept of the proposed chart is based on a good estimator of the standard deviation. Following the traditional control chart proposed by Shewhart (Montgomery, 2020), the general model of the proposed control chart is given in equation (4), where μ_{X_t} is estimated from $\hat{x}_t$ using Equation (1), whereas the σ_{X_t} estimator is obtained from Equation (3), and L is the constant that defines the distance of the control limits from the center line in terms of standard deviation units. In this context, UCL, LCL, and CL refer to the upper control limit, lower control limit, and center line, respectively.

$$\begin{aligned}\text{UCL} &= \mu_{X_t} + L\sigma_{X_t} \\ \text{CL} &= \mu_{X_t} \\ \text{LCL} &= \mu_{X_t} - L\sigma_{X_t}\end{aligned} \tag{4}$$

A schematic procedure for constructing the proposed control chart is shown in Figure 1. The procedure is described as follows:

Step 1: Collect data and input. A data set of blood glucose levels (autocorrelated) are obtained from SMBG measurements in mg/dL.

Step 2: Estimate the correlation coefficients of the model, i.e., $\delta, \phi_1, \theta_1, \varepsilon_t$, and σ_{X_t}.

Step 3: The control chart limits of the time-series control chart based on σ_{ARMA} are constructed as in Equation (4).

Step 4: Apply the proposed chart for detecting the abnormality of the blood glucose level and analyze.

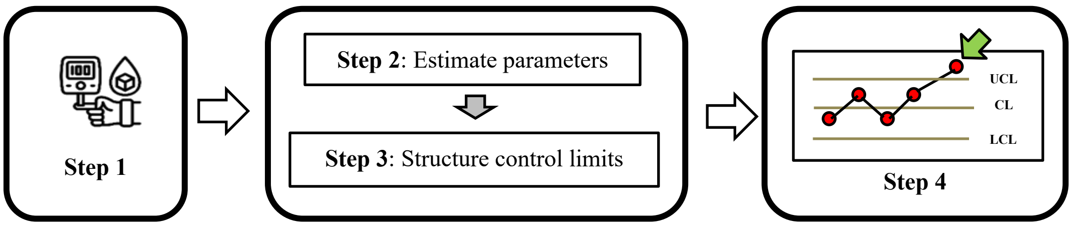

Figure 1. Schematic procedure for constructing the proposed control chart

The performance of the proposed chart is evaluated by comparing its ARL values with those of two existing approaches: (i) traditional control chart for pure residuals (i.e., the residual control chart) and (ii) a time-series control chart based on MAD. Both methods utilize the Box–Jenkins model to filter out the autocorrelation, leaving only the pure residuals for monitoring via a Shewhart chart, as shown in Equation (5) (Montgomery, 2020). This process removes predictable noise from the data, allowing the chart to focus solely on unexpected signals that indicate faults, thereby enabling faster detection of real problems (Tsai and Chen, 2009). In contrast, the second approach applies time-series control charts directly to autocorrelated data sets that fit the Box–Jenkins model. The core idea is to capture the autocorrelation structure through appropriate modeling and estimate the standard deviation using MAD. Siqueira *et al*. (2015) proposed such a chart based on a forecasting model, as illustrated in the following Equation (6).

$$\begin{aligned}\text{UCL} &= \bar{x} + L(\overline{MR}/d_2) \\ \text{CL} &= \bar{x} \\ \text{LCL} &= \bar{x} - L(\overline{MR}/d_2)\end{aligned} \tag{5}$$

$$\begin{aligned}\text{UCL} &= \hat{x}_t + L_{\text{MAD}} \\ \text{CL} &= \hat{x}_t \\ \text{LCL} &= \hat{x}_t - L_{\text{MAD}}\end{aligned} \tag{6}$$

In this context, the average of all individual observations is denoted by $\bar{x}$, and the average moving range of two consecutive observations is represented by $\overline{MR}$. A constant dependent on the subgroup size *n* is denoted by d_2. The forecasted value at time *t*, denoted by $\hat{x}_t$, is obtained from the Box–Jenkins model, as shown in Equation (1).

3. RESULTS

To evaluate the proposed chart, the ARL is calculated and then compared with that of existing approaches: the residual chart in Equation (5) and the time-series control chart based on MAD in Equation (6). The Monte Carlo simulations evaluate the ARL using ARMA (1, 1) data with unequal correlation coefficients, i.e., $\phi \neq \theta$, varied from 0.25 to 0.99 (in 0.25 increments) and sudden shifts (δ) from 0.00 to 1.00 (in 0.25 increments). Detecting small shifts enables faster intervention. Each scenario runs 10,000 replications, with in-control ARL_0 set near 370 for fair comparison. A large number of replications improves the precision and reliability of ARL estimates, as emphasized by Montgomery (2020), who noted that adequate replications are essential for accurate control chart performance evaluation. MATLAB R2023b conducts statistical analyses, and charts are prepared using Excel 365. The numerical results of the ARL are shown in Figure 2, which presents graphical results with the *x*-axis representing the magnitude of the process shift. The *y*-axis shows the ARL, which is the average number of runs required for detection, as the shift magnitude increases by unit steps on the *x*-axis.

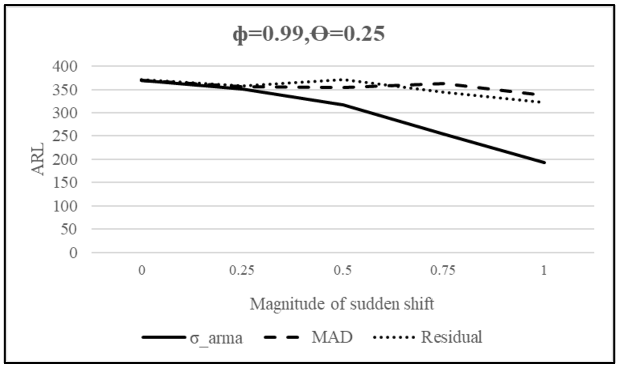
ϕ=0.99,ϴ=0.25
ARL
Magnitude of sudden shift
σ_arma
MAD
Residual

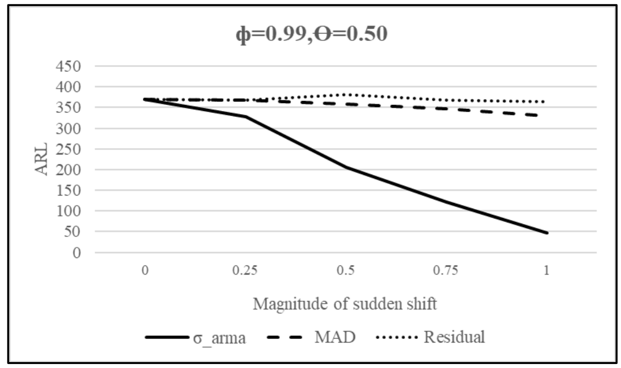
ϕ=0.99,ϴ=0.50
ARL
Magnitude of sudden shift
σ_arma
MAD
Residual

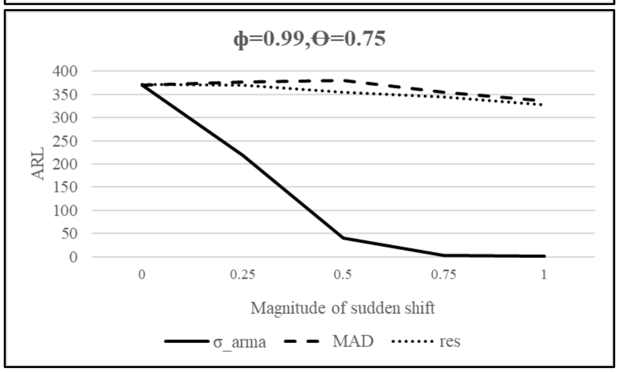
ϕ=0.99,ϴ=0.75
ARL
Magnitude of sudden shift
σ_arma
MAD
res

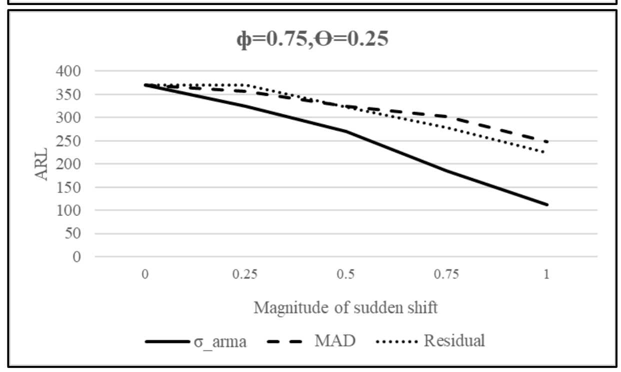
ϕ=0.75,ϴ=0.25
ARL
Magnitude of sudden shift
σ_arma
MAD
Residual

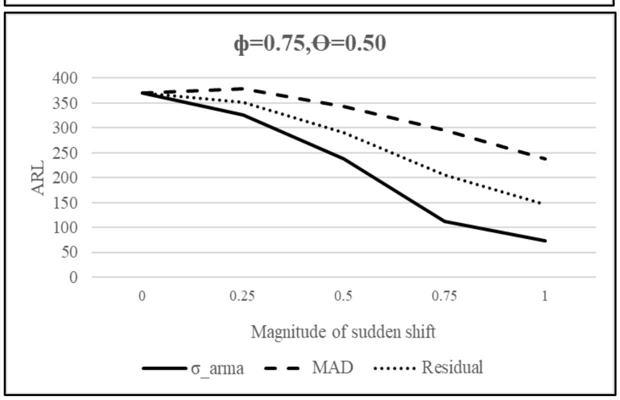
ϕ=0.75,ϴ=0.50
ARL
Magnitude of sudden shift
σ_arma
MAD
Residual

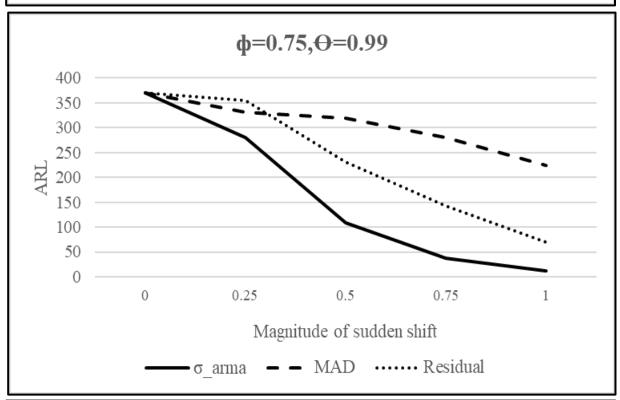
ϕ=0.75,ϴ=0.99
ARL
Magnitude of sudden shift
σ_arma
MAD
Residual

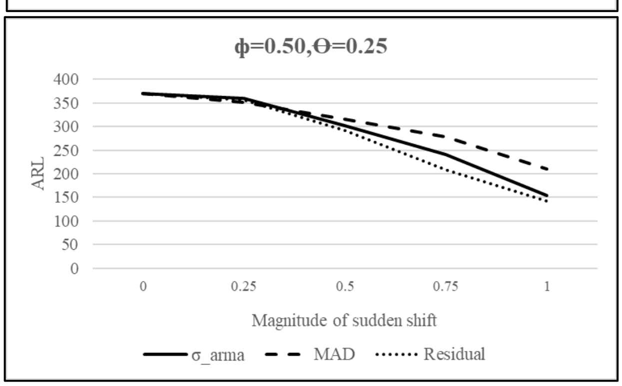
ϕ=0.50,ϴ=0.25
ARL
Magnitude of sudden shift
σ_arma
MAD
Residual

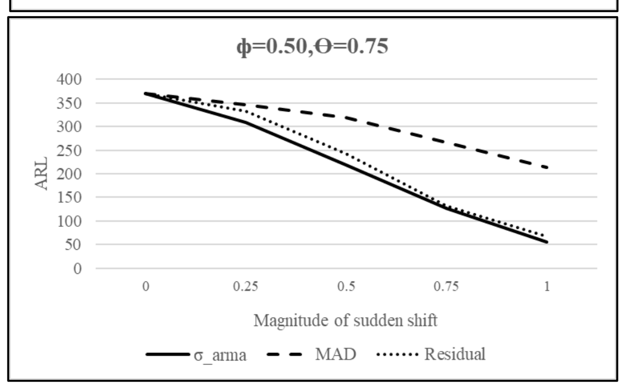
ϕ=0.50,ϴ=0.75
ARL
Magnitude of sudden shift
σ_arma
MAD
Residual

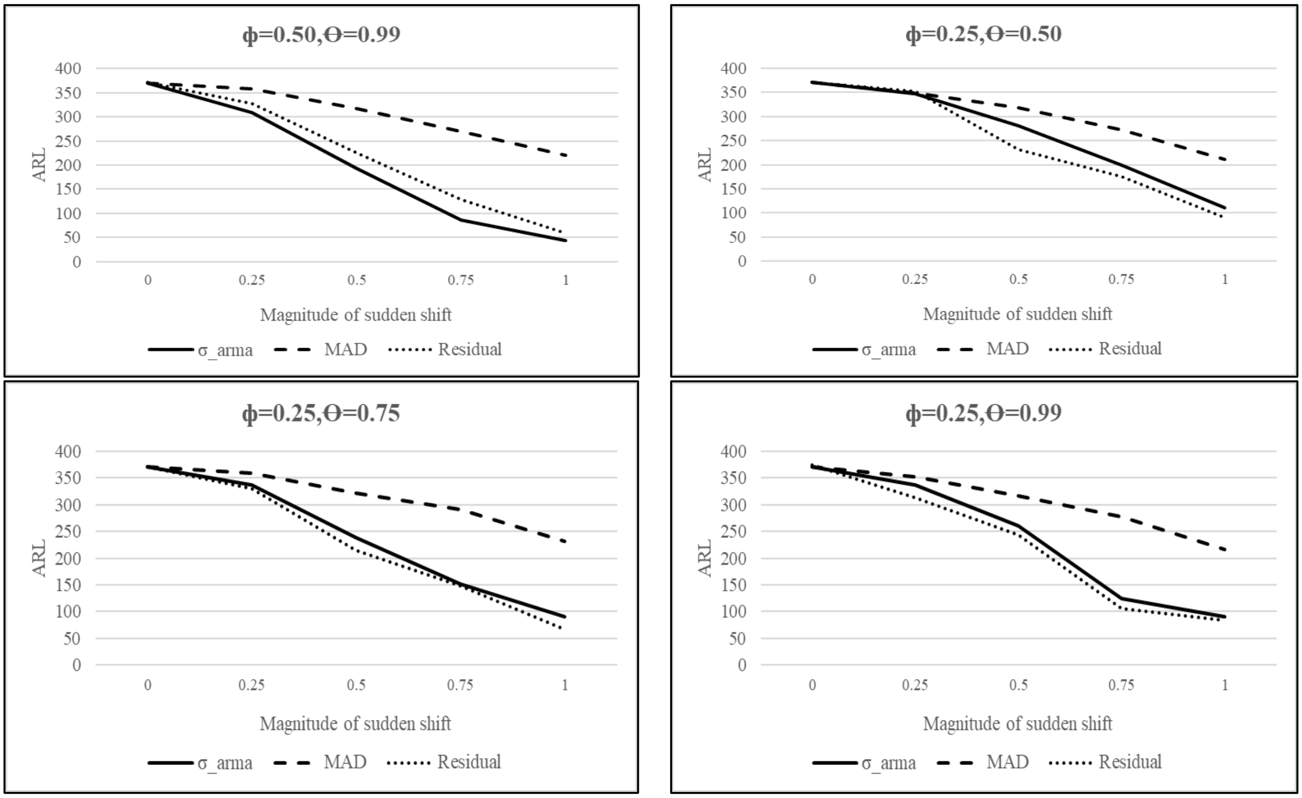

Figure 2. Comparison of the charts when parameters are varied ($\phi \neq \theta$)

In Figure 2, at ϕ= 0.99 and all values of θ, the proposed chart performs at the smallest values of ARL for all magnitude levels of the sudden shifts. A smaller ARL reflects the capability to detect abnormal events or behavioral changes more quickly; thus, it indicates a more effective control chart compared to others (Chen *et al*., 2011). Considering the performance of the residual chart and the time-series control chart based on MAD, the plotted lines of the residual chart show similar levels of ARL for all sudden shift levels, illustrating comparable performance. At $\phi = 0.75$ and all values of θ, the proposed chart is still the quickest chart to detect the abnormality, whereas at $\theta = 0.50$ and 0.99, the performance of the residual chart is quicker in detecting compared to the time-series control chart based on MAD. As observed at $\phi = 0.50$ and 0.25 for all values of θ, the ARL values and plotted lines of the proposed chart closely align with those of the residual chart, demonstrating comparable performance. Both charts outperform the time-series control chart based on MAD across all shift levels, ranging from a small shift of 0.25 to a larger shift of 1.00. These detailed observations are further summarized as the ranking performance of charts in Table 1.

Table 1 summarizes the performance of all charts in detecting abnormal events. It ranks the control charts based on ARL values under different shift sizes and ARMA (1, 1) parameter pairs (ϕ, θ), providing a comprehensive overview of their effectiveness in autocorrelated data. Since some charts exhibit comparable detection capability, multiple charts may share the same rank. Although the differences in sensitivity are relatively small, this ranking facilitates the comparison and selection of the most suitable chart. Bold numbers indicate the quickest detection (i.e., the lowest ARL) for each ϕ, θ combination paired at a given shift size.

The numerical and graphical results demonstrate the overall comparison of the three approaches based on ARL values, showing that the proposed chart provides good performance for all magnitudes of mean process change, even when the model parameters vary. In addition, the proposed chart is the quickest in detecting a shift, which means that, when abnormal behavior occurs, the proposed chart can detect even the slightest abnormality. Although some ARL results suggest that the residual chart performs slightly better, the differences are minimal. Considering the overall performance, the proposed chart demonstrates high effectiveness and sensitivity, making it capable of promptly detecting even minor abnormalities. This characteristic is particularly important for monitoring critical values, such as health-related indices like blood glucose levels, where early detection of small shifts can be vital.

Table 1. Performance summary of the control charts based on ARL values

ϕ_1	θ_1	$\delta = 0.0$			$\delta = 0.25$			$\delta = 0.50$			$\delta = 0.75$			$\delta = 1.00$		
		TS − σ_{ARMA}	TS-MAD	Res	TS − σ_{ARMA}	TS-MAD	Res	TS − σ_{ARMA}	TS-MAD	Res	TS − σ_{ARMA}	TS-MAD	Res	TS − σ_{ARMA}	TS-MAD	Res
0.99	0.25	370.0	370.5	370.9	**351.3**	355.6	370.9	**317.1**	355.1	377.6	**254.1**	362.9	372.5	**192.7**	337.6	361.5
	0.50	370.9	370.7	370.7	**328.0**	368.1	368.8	**206.7**	359.0	382.4	**121.9**	348.1	368.8	**46.2**	329.3	363.6
	0.75	370.4	370.6	370.9	**219.4**	377.4	369.7	**40.6**	380.7	354.9	**3.2**	353.9	344.5	**1.4**	335.9	326.8
0.75	0.25	370.9	370.1	370.2	**324.9**	357.3	369.9	**269.8**	324.5	322.2	**185.7**	303.1	278.4	**112.1**	248.4	223.6
	0.50	370.2	370.6	370.2	**325.7**	378.3	350.8	**237.4**	343.6	289.8	**111.4**	295.9	204.9	**73.4**	237.6	146.2
	0.99	370.9	370.3	370.4	**280.1**	330.6	354.2	**108.2**	318.6	231.2	**36.8**	279.6	143.4	**11.9**	224.2	69.1
0.50	0.25	370.7	370.3	370.6	359.7	**350.5**	356.1	301.2	315.8	**292.1**	240.6	278.4	**208.5**	174.2	211.0	**141.9**
	0.75	370.7	370.7	370.6	**309.1**	346.7	332.1	**218.7**	318.2	243.4	**127.5**	266.8	131.9	**55.6**	213.4	67.4
	0.99	370.4	370.7	370.9	**308.9**	358.8	327.5	**193.9**	316.6	224.8	**86.5**	270.1	128.3	**43.4**	220.0	59.7
0.25	0.50	370.9	370.6	370.3	**346.9**	348.8	351.3	280.7	317.7	**231.6**	199.8	272.3	**125.3**	110.7	210.9	**89.9**
	0.75	370.2	370.0	370.5	337.1	358.1	**329.9**	237.9	322.1	**215.0**	151.4	291.4	**118.4**	89.7	231.7	**66.5**
	0.99	370.3	370.1	374.3	337.7	351.7	**313.8**	260.8	316.9	**213.9**	125.0	278.0	**106.7**	90.3	215.9	**53.6**

*Charts include time series based on σ_{ARMA} (TS − σ_{ARMA}), time series based on MAD (TS-MAD), and residual (Res).
*Results of the control chart that provides quick detection for each shift size under different ARMA (1, 1) parameter settings are highlighted.
*The ARL values in bold represent the quickest detection in each condition to make the comparison explicit.

4. A CASE STUDY

The focus of this paper is applying the proposed chart in practice using SMBG data from patients with T2D obtained from the University of California Irvine or UCI repository (Kahn, n.d.). Figure 3 presents a flowchart of the practical implementation steps for using the proposed chart. Fasting blood glucose (FBG) levels, which were measured from a patient's blood sample on a given day, are plotted on the chart, analyzed, and interpreted to identify the root cause of any abnormalities. This process enables guideline-based treatment, lifestyle modification, and self-management. Continuous application, along with iterative behavioral adjustments, is expected to further improve the long-term outcomes for patients with diabetes. Figure 4 illustrates the results from using the proposed control chart for monitoring FBG data. In the figure, the x-axis represents the days of FBG measurement, and the y-axis shows the FBG levels (in mg/dL) recorded from SMBG. The upper, middle, and lower gray lines indicate the UCL, CL, and LCL, respectively, whereas the black line represents the actual FBG values.

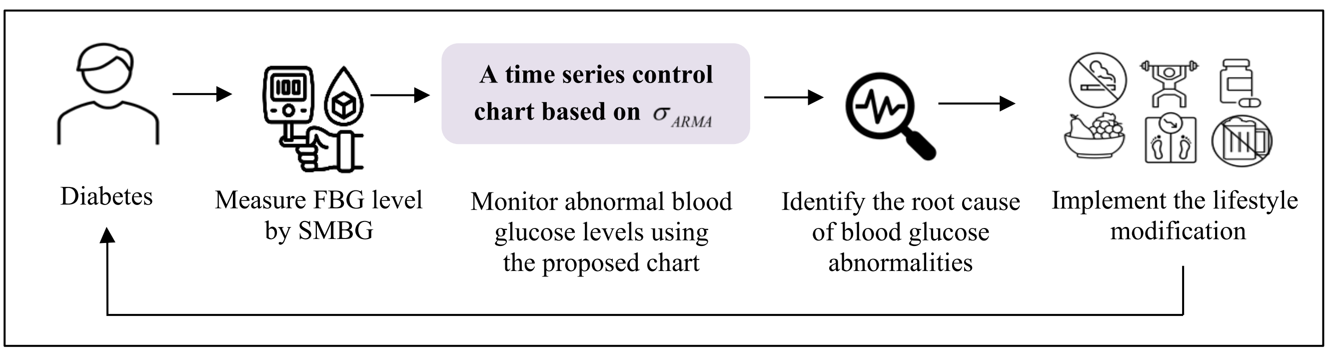

Figure 3. Flowchart of implementation steps for the practical

In Figure 4, three points exceeding the UCL were identified. Upon detecting out-of-control or abnormal blood glucose levels, the initial step should be to determine the root cause, which often reflects the patient's lifestyle and behavior. Despite some fluctuations, the overall control of FBG levels is relatively good. Observing from a long-term evaluation over 90 days reveals that only three points exceeded the UCL. However, considering that the average FBG level of plotted points is approximately 159 mg/dL, which remains still high (i.e., greater than 126 mg/dL), patients still need to modify their behavior to keep their blood glucose levels lower. Identifying the causes of out-of-control points provides patients with valuable lessons in modifying their previous behavior and awareness in life. Diabetes can lead to several associated consequences, such as amputation of the lower extremities, neuropathy, renal disease, cardiovascular disease, and blindness (Deshpande, 2008). In particular, if the FBG level is greater than 250 mg/dL, the possibility of excessively high levels indicates an urgent emergency, which may result in a life-threatening diabetic coma. As such, if a patient's lifestyle habits remain unchanged and cannot be controlled, insulin is often recommended as the first-line treatment for symptomatic or severe hyperglycemia. This means that the patient may have to rely on insulin indefinitely, which can feel like a loss of lifestyle flexibility compared to managing with oral medications along with lifestyle modifications. According to the American Diabetes Association (American Diabetes Association Professional Practice Committee, 2022), regular exercise reduces blood glucose levels; however, patients with T2D may adhere to the exercise guidelines proposed by Batrakoulis *et al*. (2022), in which unbalanced exercise is a caution.

In addition, in the case that plotted points are outside both upper and lower control limits, this indicates an out-of-control situation relating to the occurrence of glycemic variability. Reducing the fluctuation in the blood glucose level to further minimize fluctuations should be considered in self-management through lifestyle modifications and continuous blood glucose monitoring. Watts *et al*. (2011) provided a summary of blood glucose pattern evaluation rules and guidelines for self-management according to each rule. As can be seen, the results of utilizing the proposed control charts for detecting abnormal blood glucose levels in diabetics could encourage patients to raise awareness of their condition and lead to changes in lifestyle behaviors, thus promoting self-management.

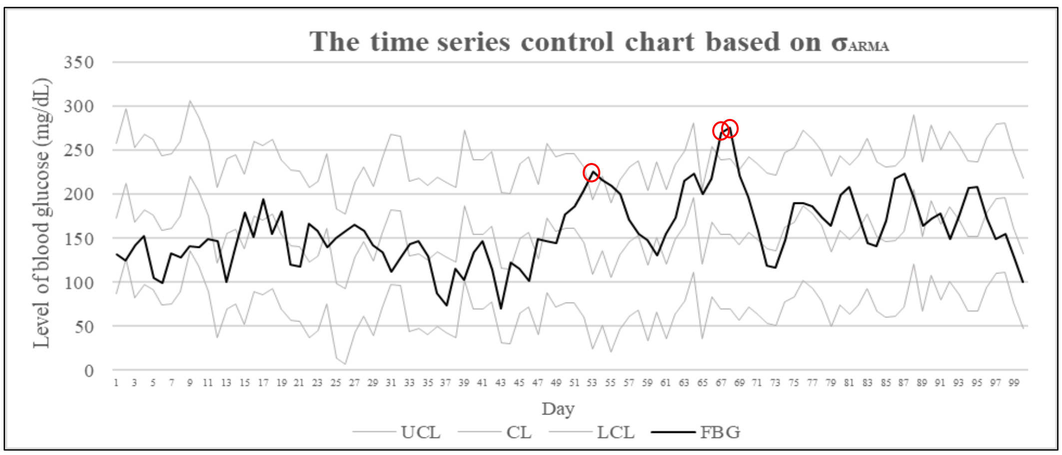

Figure 4. Using the proposed control chart for monitoring FBG data

5. DISCUSSION

This study highlights the importance of monitoring diabetes-related behaviors by analyzing fluctuations in blood glucose levels, which serve as indicators of patients' self-management practices. Traditional diabetes monitoring primarily relies on control charts based on the assumption of IID data. However, given that blood glucose levels often exhibit autocorrelation, conventional control charts may not be suitable for tracking such data patterns. To address this gap, a proposed chart utilizing a robust estimator is proposed, which demonstrates superior or comparable performance to residual charts and time-series control charts based on MAD. The proposed chart efficiently detects small fluctuations and is applicable to other autocorrelated health indices. The proposed chart is quickest in detecting abnormalities when the data are highly correlated. In medium-to-low correlation scenarios, the proposed chart performs similarly to the traditional chart. Results indicate that the proposed chart rapidly identifies even the slightest abnormalities in blood glucose levels across all correlation ranges.

Application to real SMBG data confirms the chart's capability in detecting subtle changes rapidly and facilitate behavioral interventions aligned with clinical guidelines. This enhances patient awareness and promotes timely behavior modifications, reinforcing treatment adherence. Accordingly, the proposed methodology offers adaptability to a wide range of autocorrelated data sets beyond healthcare applications. The capability to detect structured dependencies in varied data presents benefits across multiple fields, including finance, environmental monitoring, and industrial quality control. However, its implementation in healthcare is particularly crucial, since early detection directly affects patient outcomes by enabling timely medical interventions. Nevertheless, this study primarily focuses on positive autocorrelation structures. Future research should explore its effectiveness under different correlation conditions, such as negative or mixed autocorrelation, which can be commonly found in real-world healthcare settings. Furthermore, integrating advanced statistical models, predictive analytics, and real-time monitoring systems can enhance the applicability of this approach, supporting broader implementation across various domains while optimizing diabetes management strategies.

6. CONCLUSION

Within Given the increasing prevalence of diabetes, the continuous monitoring of blood glucose levels is crucial for early detection and intervention. The findings have demonstrated that the proposed control chart effectively identifies abnormalities and provides meaningful behavioral feedback. The chart sensitivity enables the early detection of irregularities, reinforcing self-awareness and adherence to lifestyle modifications. By integrating statistical monitoring with patient behavior, the proposed approach offers a practical tool for improving diabetes care. Likewise, it helps to encourage patients to be careful with their behavior and apply lifestyle modifications that enhance the practical applicability of managing diabetes, providing better treatment for patients.

REFERENCES

American Diabetes Association Professional Practice Committee. (2022). 5. Facilitating Behavior Change and Well-being to Improve Health Outcomes: Standards of Medical Care in Diabetes-2022. *Diabetes Care*, 45: S60–S82.

American Diabetes Association Professional Practice Committee. (2025). Improving Care and Promoting Health in Populations: Standards of Care in Diabetes—2025. *Diabetes Care*, 48(Supplement_1): S14–S26.

Aslam, M., Khan, N., and Albassam, M. (2024). Designing a Control Chart for Gamma Distribution through Repetitive Sampling with Imprecise Data. *International Journal of Industrial Engineering: Theory, Applications and Practice*, 31(6).

Aslam, M., Rao, G. S., Khan, N., and Al-Abbasi, F.A. (2019). EWMA Control Chart Using Repetitive Sampling for Monitoring Blood Glucose Levels in Type-II Diabetes Patients. *Symmetry*, 11(1), 57.

Atieno Wagoro, M. C., Sudi Galo, W., Rakuom, C. P., Oderah Mirereh, J., and Musee, C. (2020). Development of a graphic blood glucose monitoring chart for glycaemic control in diabetes mellitus: a modified Delphi method study. *Journal of Research in Nursing*, 25(4), 323–344.

Babatunde, S.A., Odeyemi, O., and Babatunde, A.M. (2020). Showcasing the Properties of a Good Estimator; Using Practical Empirical Illustrations. *Journal of Probability Section of Teaching and Applications and Statistical Science*, 18:177–186.

Batrakoulis, A., Jamurtas, T., and Fatouros, I. (2022). Exercise and Type II Diabetes Mellitus: A Brief Guide for Exercise Professionals. *Strength and Conditioning Journal*, 44:64–72.

Box, G.E.P., Jenkins, G.M., Reinsel, G.C., and Ljung, G.M. (2016). *Time Series Analysis* (5th ed.). New Jersey: John Wiley & Sons.

Chen, L.-H., Chang, F. M., and Chen, Y.-L. (2011). The application of the multinomial control charts under inspection error. *International Journal of Industrial Engineering: Theory, Applications and Practice*, *18*(5).

Deshpande, A.D., Harris-Hayes, M., and Schootman, M. (2008). Epidemiology of diabetes and diabetes-related complications. *Physical Therapy & Rehabilitation Journal*, 88:1254–1264.

Faria, S.C.E., Jardim, F.S., Camargo, V.C.B., Lizarelli, F.L., and Oprime, P.C. (2020). Unconditional performance of the $\bar{X}$ chart: Comparison among five standard deviation estimators. *Quality and Reliability Engineering International*, 36:1808–1819.

Hamm, N., Marrie, R.A., Jiang, D., Irani, P., and Lix, L. (2024). Trend control charts for multiple sclerosis case definitions. *International Journal of Population Data Science*, 9(1).

Haridy, S. and Benneyan, J.C. (2024). Shewhart-type control charts for monitoring binomial data subject to shifts of random amounts. *Computers & Industrial Engineering*, 193, 110252.

IDF Diabetes Atlas, 11th Edition Committee. (2025). *IDF Diabetes Atlas 10th edition*. Brussels: International Diabetes Federation.

Kahn, M. (n.d.). Diabetes data set. UCI Machine Learning Repository. https://archive.ics.uci.edu/ml/datasets/Diabetes

Kao, S.-C. (2013). Monitoring turnaround time using an average control chart in the laboratory. *International Journal of Industrial Engineering: Theory, Applications and Practice*, *19*(12).

Kuntapa, N., and Purintrapiban, U. (2019). Selection of control chart for monitoring blood glucose level. *Proceedings of the Asia Pacific Industrial Engineering & Management Systems Conference*, Kanazawa, Japan.

Montgomery, D. C. (2020). *Introduction to Statistical Quality Control* (8th ed.). John Wiley & Sons.

Pakdil, F., Azadeh-Fard, N., and Esatoglu, A.E. (2019). Monitoring length of stay through control charts: a comparative study of diabetic patients. *Hospital Practice (1995)*, 47(4):196–202.

Prajapati, D.R., and Singh, S. (2012). Control charts for monitoring the autocorrelated process parameters: A literature review. *International Journal of Productivity and Quality Management*, 10:207–249.

Sapkota, R.P., Upadhyaya, T., Gurung, G., Parker, M., Raman, R., and Pardhan, S. (2018). Need to improve awareness and treatment compliance in high-risk patients for diabetic complications in Nepal. *BMJ Open Diabetes Research & Care*, 6: e000525.

Siqueira, J., Nunes, A., Ferreira, M., Linhares, A., Ramos, E., and Gabbay, Y. (2015). Application of time series control charts to model and monitor the seasonality of norovirus. *Revista Pan-Amazônica de Saúde*, 6:61–68.

Tsai, T.-N., and Chen, L.-H. (2009). Monitoring of the stencil printing process using a modified regression residual control chart: an empirical study. *International Journal of Industrial Engineering: Theory, Applications and Practice*, *16*(4).

Watts, S., Lawrence, R., and Kern, E. (2011). Diabetes Nurse Case Management Training Program: Enhancing Care Consistent with Chronic Care and Patient-Centered Medical Home Models. *Clinical Diabetes*, 29:25–33.

Yager, R.R., and Alajlan, N. (2014). A note on mean absolute deviation. *Information Sciences*, 279:632–641.